

1 **Impact of processing conditions on microstructure, texture and chemical properties of**
2 **model cheese from sheep milk**

3 Ane Aldalur^{acd}, Lydia Ong^{bcd}, María Ángeles Bustamante^a, Sally L. Gras^{bcd**}, Luis Javier R.
4 Barron^{a*}

5 ^a Lactiker Research Group, Faculty of Pharmacy, University of the Basque Country (UPV/EHU),
6 Paseo de la Universidad 7, 01006-Vitoria-Gasteiz, Spain.

7 ^b Department of Chemical Engineering, The University of Melbourne, Parkville, Vic 3010,
8 Australia.

9 ^c The Bio21 Molecular Science and Biotechnology Institute, The University of Melbourne,
10 Parkville, Vic 3010, Australia

11 ^d The ARC Dairy Innovation Hub, Department of Chemical Engineering, The University of
12 Melbourne, Parkville, Vic 3010, Australia

13 * Corresponding author: luisjavier.rbarron@ehu.eus

14 ** Co-corresponding author: sgras@unimelb.edu.au

15 **Abstract**

16 Cutting and cooking settings have a strong effect on curd particle features, whey syneresis and
17 cheese properties. In the present study, the impact of curd grain size and cooking temperature on
18 the microstructure, texture and composition of cheese, whey losses and cheese yield was studied
19 with specific focus on sheep milk. Cooking temperature especially affected cheese
20 microstructure, texture and composition, while cutting process was largely responsible for fat
21 losses in the whey. Additionally, cheese yield increased with a bigger curd grain size and lower
22 cooking temperatures. Higher cooking temperatures reduced the moisture content of the curd
23 grains and cheese and lead to cheeses with reduced porosity and more free fat in their structure,
24 resulting in harder and chewier cheeses. Interactions between the microstructural arrangement of
25 fat and textural parameters were also observed. These results contribute with new data on the
26 relationships between curd grain size and cooking conditions on the microstructure and physico-
27 chemical properties of cheese. In addition, reducing the compound losses in whey would have a
28 direct effect on the improvement of processing, cheese quality and yield, and the ulterior
29 byproduct management.

30 **Keywords:** Confocal microscopy, cryo-scanning electron microscopy, fat loss, curd grain size,
31 cooking temperature, cheesemaking settings.

32

33 **Highlights**

- 34 • Cutting and cooking settings affect cheese microstructure and texture properties
- 35 • A higher cooking temperature raised free fat formation and reduced cheese porosity
- 36 • The hardness and chewiness of cheese increased with higher cooking temperature
- 37 • A bigger curd grain size increased the globular fat volume in cheese microstructure
- 38 • A smaller curd grain size enhanced the fat loss and decreased cheese yield

39 **1. Introduction**

40 The technological conditions used during cheese processing, particularly curd cutting and cooking
41 process, have a direct effect on cheese composition, yield and compound losses in the whey.
42 During cutting and cooking, syneresis of curd occurs and this is affected by several factors well
43 documented in the scientific literature such as: milk composition, firmness of the gel at cutting,
44 gel acidity, temperature, time of cutting, speed of rotation of the cutting and stirring tools and the
45 surface area of the curd (Banks 2007; Dejmek and Walstra 2004; Everard et al. 2008; Johnston et
46 al. 1991; Johnston et al. 1998; Walstra et al. 2006).

47 While some authors (Johnston et al. 1991; Whitehead and Harkness 1954) have suggested that
48 the size of the curd grain plays an important role in the moisture of the final cheese product, others
49 have found that different curd cutting intensities have little effect on the extent of syneresis,
50 although enhanced losses of fat and casein fines were reported (Everard et al. 2008). The
51 relationship between fat and protein losses from the curd and a reduction in cheese yield with
52 curd grain size has been shown to be influenced not only by the cutting revolutions but by a
53 combination of the total revolutions applied during cutting and cooking processes (Everard et al.
54 2008; Johnston et al. 1991; Johnston et al. 1998). Even though cheesemaking processing
55 conditions affect chemical properties of cheese, the studies about the interactions of cutting and
56 cooking settings with microstructure and texture are scarce. Additionally, the comparison of
57 cutting and stirring conditions in this prior studies is made difficult due to technical differences
58 in the cheesemaking processes applied. In this study, the curd grain size was assessed by image
59 analysis to provide information about the curd grain size obtained at the end of the cutting or
60 cooking processes (Aldalur et al. 2019). This method may reduce some of the comparative issues
61 described by other authors, such as the use of different vat designs and sizes, cutting knives,
62 stirrers and cutting and stirring conditions (Everard et al. 2008; Johnston et al. 1998).

63 Temperature is another factor that enhances moisture expulsion from curd grains, as the
64 permeability of the curd matrix increases at higher temperatures (Fagan et al. 2007). A rapid

65 increase in temperature, however, may lead to a shrunken outer layer of the curd grain, impairing
66 permeability and slowing syneresis (Dejmek and Walstra 2004). Moreover, temperature greatly
67 affects the properties of fat globules and the spatial arrangement of other components in cheese,
68 which ultimately determine the structure of the cheese and its physico-chemical and sensory
69 properties (Lamichhane et al. 2018; Lopez et al. 2006). As a result, the microstructural
70 observation of cheese and samples taken during the cheesemaking process can be very useful to
71 predict and control the properties of the final cheese product (El-Bakry and Sheehan 2014).
72 Confocal laser scanning microscopy (CLSM) is a powerful tool, which allows two-dimensional
73 (2D) thin optical sections of a sample to be digitally captured and reassembled to obtain three-
74 dimensional (3D) information (Gunasekaran and Ding 1998). This imaging allows both fat and
75 protein to be visualised and quantified, providing numerical information about the size, shape and
76 distribution of key components of the curd and cheese matrix. In addition, cryo-scanning electron
77 microscopy (cryo-SEM) provides a detailed image of the surface features of hydrated samples
78 without chemical staining and conventional sample drying (Ong et al. 2011).

79 Cheese produced from raw sheep milk is particularly important in European countries such as
80 France, Italy, Greece, Spain and Romania (EUROSTAT 2016). This type of milk is suitable for
81 cheesemaking due to the higher concentration of milk components and improved coagulation
82 properties compared to cow milk (Kammerlehner 2009; Park et al. 2007). While considerable
83 differences have been observed, the effects of the conditions used during the cheesemaking
84 process using sheep milk in the cheese product, compound losses and yield have been scarcely
85 reported.

86 The objective of the current study was to investigate the effect of the processing parameters curd
87 grain size, assessed by image analysis, and cooking temperature on the microstructure, texture,
88 composition and yield of cheese from sheep milk.

89 **2. Materials and methods**

90 *2.1. Experimental design and sampling*

91 A two-level full factorial experimental design was employed, which looked at the effects of curd
92 grain size (*CGS*) and cooking temperature (*CT*) on the final cheese product (Table 1). Two levels
93 of *CGS* were selected: big and small, and two levels of *CT*: 36 °C and 45 °C, all other
94 cheesemaking conditions remained fixed. The four experimental cheeses were made in two
95 consecutive days using the same bulk raw ewe milk collected from a local farm (Meredith Dairy,
96 Truganina, Victoria, Australia) one day prior to the first day of cheesemaking. Simultaneous
97 treatments were carried out in two identical vats. On the first day the big *CGS* factor level was
98 selected and the *CT* factor was varied in the two identical vats. The following day, the same
99 procedure was followed except the *CGS* factor level selected was small. The experiments were
100 then replicated the following week using a second collection of bulk milk. [Online Resource 1](#)
101 summarises the most relevant physico-chemical and rheological parameters of the milk used for
102 the experimental cheesemaking.

103 Cheese production was carried out in a small cheesemaking facility located at The Bio21
104 Molecular Science and Biotechnology Institute (The University of Melbourne, Melbourne,
105 Australia). The cheesemaking process carried out was a typical manufacture of semi-hard sheep
106 cheeses which are usually ripened for a minimum of 2 months. For that purpose, 20 L cubic-
107 shaped stainless-steel double jacketed open vats were used. Each experimental cheese was made
108 using 10 kg of raw sheep milk, which was stored at 5 °C for 1 or 2 d before cheese production.
109 First, the cheese milk was tempered to 25 °C in the vat with constant stirring at 30 rpm for ~35
110 min before adding 0.02 g/kg of freeze-dried mesophilic starter culture, *Lactococcus lactis*, subsp.
111 *lactis* and *Lactococcus lactis* subsp. *Cremoris* (Danisco, Copenhagen, Denmark). The
112 temperature was increased from 25 °C to 30 °C over 20 min and 0.03 g/kg of rennet (IMCU ~1400,
113 Hansen Naturem, Chr. Hansen, Hørsholm, Denmark) added. Stirring was stopped 2 min after
114 rennet addition to ensure the correct blending of the mixture. The cutting time was set to 40 min
115 after rennet addition and the gel strength of each batch was determined at this time point. Cutting
116 was performed using two manual cheese cutting frames with nylon wires (Grunt, Victoria,
117 Australia) stretching in the horizontal (29 wires) or vertical direction (23 wires). The spacing

118 between the wires in both directions was 1 cm. First, both cutting frames were inserted in the left
119 side of the vat and moved simultaneously from left to right once and removed. The two frames
120 were then inserted again at the back of the vat and were pushed through the curds to the front of
121 the vat. This whole movement was repeated either twice to obtain big curd grains or six times to
122 obtain small curd grains. The assessment of the curd grain size (big and small) was performed
123 after cutting and stirring (Table 1) by image analysis, as previously reported (Aldalur et al. 2019)
124 to ensure that two well defined and significantly different curd grain sizes were produced during
125 cheesemaking. After cutting, the curd grain and whey mixture was stirred at 40 rpm for 50 min
126 while the temperature increased from 30 °C to either 36 °C or 45 °C, depending on the *CT* selected.
127 The cooking temperature rate was different for both *CT*, with mean values of 0.12 and 0.30 °C/min
128 when the temperature was raised to 36 °C and 45 °C, respectively. Whey was then drained from
129 the vat and weighed. The curd was placed manually into a metallic cheese mould with a wet cloth
130 and pressed at 4.2 kg/cm² in a horizontal hydraulic press for ~4-5.5 h at room temperature (~ 20
131 °C) until the cheese pH dropped to 5.50 ± 0.07. The pressed cheese was removed from the mould
132 and weighed (± 0.5 g). The final cheese had a cylindrical shape 15 cm in diameter and ~12 cm in
133 height, with an approximate weight of 2 kg. Within this study, the brining and ripening typically
134 following cheesemaking were not carried out. The pH values at rennet addition (i.e. coagulation
135 pH), cutting, stirring, whey draining and after pressing are shown in Table 1. The cheese was
136 subsequently cut into four quarters or subsamples, vacuum packed and stored at 5 °C until
137 physico-chemical and microstructure analyses.

138 During the cheesemaking process, intermediate samples of curd, curd grains after cutting (fresh
139 curd grains, FCG), curd grains after cooking (stirred curd grains, SCG) and whey were collected.
140 For image analysis of the curd grains, FCG and SCG samples were collected using a round steel
141 mesh sieve 13 cm in diameter with 0.7 mm mesh openings. The sieve was submerged to a depth
142 approximately halfway between the top and bottom of the vat right after the end of either cutting,
143 to collect FCG or after stirring or to collect SCG, the grains were extracted by draining the excess
144 whey. For CLSM analysis, intermediate samples were stored at 5 °C for no more than 3 h. For

145 compositional analysis, curd grain samples were frozen at -30 °C until analysis. CLSM, analysis
146 to determine fat globule size and rheological analysis of milk samples was carried out on the day
147 of milk collection. Samples were then kept frozen (-30 °C) for compositional analysis.

148 2.2. *Physico-chemical analysis*

149 The fat content was determined by the Babcock method (AOAC 2005). Protein content was
150 obtained by analysing the nitrogen content using the combustion method (ISO/IDF 2002) with a
151 nitrogen determinator (TruMac CNS, LECO Corporation, Saint Joseph, MI, USA); this value was
152 then multiplied by a factor of 6.38 (ISO/IDF 2014). Dry matter (DM) was measured by drying
153 the samples overnight (ISO/IDF 2004; 2010). The pH during the cheesemaking process and in
154 the final product was assessed using a pH meter (S220 SevenCompact, Mettler Toledo, Port
155 Melbourne, Australia).

156 The total calcium, magnesium and phosphorous content of samples was analysed using
157 Inductively Coupled Plasma-Optical Emission Spectroscopy (ICP-OES) (720ES; Varian Inc.,
158 Palo Alto, CA, USA) (Chen et al. 2016). Liquid samples were prepared for the ICP-OES analysis
159 by diluting the sample 100 times in high purity water (resistivity of 18.2 mΩ·cm; Millipore,
160 Billerica, MA, USA) followed by filtering through a 0.22 µm pore size filter (Millipore). Solid
161 samples were dried overnight at 100 °C before ashing at 600 °C for 4 h using a chamber furnace
162 equipped with a temperature controller (FP93, Shimaden, Tokyo, Japan) to remove the organic
163 matter. The ashes were then dissolved in nitric acid (68%) and hydrochloric acid (32%) (1:1;
164 vol/vol; both from Univar, Ingleburn, NSW, Australia) before diluting 1000 times in high purity
165 water and filtering through a 0.22 µm pore size filter for ICP-OES analysis. All physico-chemical
166 analyses were performed in duplicate for each sample.

167 The particle size distribution of the milk fat globules was measured by Light Scattering (LS) using
168 a particle size analyser (Mastersizer 3000; Malvern Instruments, Malvern, UK), as described
169 previously by Ong et al. (2010). Briefly, sheep milk samples were diluted (1:1; vol/vol) in
170 ethylenediaminetetraacetic acid (EDTA, 50 mM, pH 7) 2 hours before analysis. Samples were

171 then added to a circulating cell containing a mixture of water and sodium dodecyl sulphate (SDS,
172 0.05%). The refractive indices of the milk fat and water were set at 1.460 and 1.334, respectively.
173 The volume weighted mean diameter $D[4,3]$ was calculated by the particle analyser software.

174 *2.3. Coagulation properties and texture*

175 The coagulation properties of the milk at renneting were analysed using a Twin Drive Rheometer
176 (MCR702, Anton Paar, North Ryde, Australia), equipped with a CC27 cup and bob accessory. A
177 sample of milk containing rennet was loaded into the cup while the temperature was maintained
178 at 30 °C. The analysis was carried out at an angular frequency of 0.8 Hz and 0.1% shear strain.
179 Changes in storage modulus (G'), loss modulus (G'') and loss factor $\tan(\delta)$ were measured every
180 10 s for 60 min. The onset of gelation (s) was defined as the time at which the G' first reached
181 0.05 Pa, the curd firming rate (Pa/s) was obtained from the maximum slope determined over 12
182 consecutive points and the final curd firmness defined as the G' value at 60 min after rennet
183 addition (Logan et al. 2014). All samples were analysed in duplicate.

184 The gel strength at the cutting point was analysed using a texture analyser (TA.HD plus; Stable
185 Micro Systems, Godalming, UK) equipped with a 5 kg load cell and a cylindrical probe (10 mm
186 diameter). Immediately after rennet addition and blending, two 50 mL samples of milk were taken
187 directly from the cheese vat, poured into a plastic container 42 mm in diameter and 55 mm in
188 height and incubated for 40 min at 30 °C. A test speed of 1 mm/s was used and the penetration
189 was set to 20 mm with a trigger force of 1g. The maximum force obtained during the penetration
190 was used as the measure of gel strength. The measurement was performed in duplicate on the two
191 samples collected for each cheese vat and the mean value of gel strength was used for each vat.

192 Texture profile analysis was carried out using the texture analyser following a published method
193 with some modifications (Ong et al. 2012). Briefly, cheese samples were taken from the centre of
194 the cheese subsample using a knife and a cylindrical cheese corer to obtain three samples 2.5 cm
195 in diameter and 2.5 cm in height. These were equilibrated at room temperature (~20 °C) for 1 h
196 in a closed container prior to analysis to prevent moisture loss. A 35 mm cylindrical flat probe

197 was used and a 50% compression test was applied to the cheese using two compression cycles at
198 a constant crosshead speed of 2 mm/s. Three analyses were performed for each cheese treatment.

199 *2.4. Determination of cheese yield*

200 The actual cheese yield (kg of cheese/100 kg of milk) per vat was estimated as the ratio of the
201 total weight of fresh cheese after pressing to the weight of milk used in the vat. Moisture-adjusted
202 cheese yield (Y_{MA}) was calculated using the equation (1) described by Guinee et al. (2006).

$$203 \quad Y_{MA} = Y_A \times ((100-M_A)/(100-M_R)) \quad (1)$$

204 where Y_A was the actual cheese yield and M_A and M_R were the actual and reference (45.0%)
205 moisture contents of the cheese, respectively. The theoretical cheese yield (Y_T) was calculated
206 using equation (2) described by Van Slyke (Emmons and Modler 2010):

$$207 \quad Y_T = (0.93 \times F + (C - 0.1)) \times 1.09 \times 100/(100 - (M)) \quad (2)$$

208 where F and C were the fat and casein content of the milk respectively and M was the desired
209 cheese moisture content, which was 45% in this instance. Casein content of milk was estimated
210 as the 80 % of the total protein (Park et al. 2007). The yield efficiency (Y_E) was calculated as the
211 percentage of the ratio between Y_{MA} and Y_T (Barbano and Sherbon 1984). The amount of fat,
212 protein and minerals lost in the whey were calculated on the basis of milk weight following
213 methods described by Guinee et al. (2006). Fat loss percentage (FL) was calculated as described
214 in equation 3:

$$215 \quad \% FL = (W_W \times W_F)/(M_W \times M_F) \times 100 \quad (3)$$

216 where W_W and M_W were the weight (kg) of the drained whey and milk, respectively and W_F and
217 M_F were the fat content (wt/wt) of whey and milk, respectively. The protein and mineral losses
218 were calculated using similar formulas described in the same reference.

219 *2.5. Microstructure analysis*

220 Milk, gel, curd grain and cheese samples were prepared for microstructural examination using
221 CLSM by applying a method reported previously (Ong et al. 2011). Briefly, solid samples were
222 cut into approximately 5 x 5 x 2 mm in size using a surgical blade and stained at ~ 4 °C using Nile
223 Red (0.1 mg/mL) (Sigma-Aldrich, Castle Hill, Australia) and fast green FCF (0.1 mg/mL)
224 (Sigma-Aldrich). For milk samples, Nile Red (0.02 mg/mL), fast green FCF (0.02 mg/mL),
225 agarose (0.5%) (Sigma-Aldrich) and milk were mixed and the stained sample was then placed on
226 a cavity slide and covered with a coverslip (0.17 mm thick) secured with nail polish (Maybelline,
227 LLC, NY, USA). Microstructural analysis was performed using an inverted confocal microscopy
228 (SP8; Leica Microsystems, Heidelberg, Germany) with excitation wavelengths of 488 nm for fat
229 and 638 nm for protein. Leica confocal software was used to acquire two-dimensional images 512
230 x 512 pixels in size.

231 Cheese samples were also analysed by cryo-SEM, as described by Ong et al. (2011). Briefly,
232 cheese samples 5 x 5 x 2 mm were placed on the sample holder and immersed into a liquid
233 nitrogen slush (-210 °C) for 10 s. The frozen samples were then transferred into the cryo
234 preparation chamber, which was maintained at -140 °C under high vacuum conditions ($< 10^{-4}$ Pa).
235 The sample was fractured horizontally using a cooled scalpel blade and etched at -95 °C for 30
236 min. The temperature was reduced to -140 °C and the cheese sample was coated with 10 mA of
237 sputtered gold/palladium alloy (60/40) using a cold magnetron sputter coater (300V) for 120 s
238 generating a layer ~ 6 nm thick. The sample was then placed onto a nitrogen gas cooled module
239 under vacuum, maintained at -140 °C and observed using a field emission SEM (Quanta; Fei
240 Company, Hillsboro, OR, USA) with a spot size of 2 and acceleration voltage of 15 kV. The
241 detector used for observation was a solid-state backscattered electron detector.

242 *2.6. Image analysis*

243 Three-dimensional (3D) image analysis was carried out for the CLSM micrographs of milk, curd,
244 curd grains and cheese samples. For each sample, a minimum of 30 adjacent planes were acquired
245 with a separation of 0.5 μm and reconstructed for an observation depth of 15 μm . This 3D

246 reconstruction was carried out using ImageJ software (National Institutes of Health, Bethesda,
247 MD, USA). First, the 2D image layers were stacked together to reconstruct the 3D image. Stacks
248 were equalized using Stack Normalizer plug-in and the channels were split to separate the data
249 for fat and protein. For both stacks, the background was subtracted to enhance image quality. For
250 the fat micrograph stack, a 3D Median filter was also used to smooth the image and improve
251 analysis. The stacks were then thresholded using the IsoData thresholding method (Ridler and
252 Calvard 1978). A Watershed function was applied to separate fat globules that appeared coalesced
253 in the samples. To quantify image features, a 3D Object Counter was used to obtain volume and
254 area surface measurements. This procedure allowed the fat globule diameter and sphericity to be
255 determined together with the network porosity. In addition, two distinct populations of fat
256 globules were identified in samples that were quantified by image analysis. These were the
257 population of globular fat droplets and the population of non-globular or coalesced fat droplets.
258 Globular fat droplets were defined as those droplets with a diameter smaller than the mean
259 diameter of the fat globule in milk. The diameter of these fat droplets ranged from 0.57 to 5.93
260 μm , which were clearly not disrupted by the handling encountered during the cheesemaking
261 process. Non-globular fat droplets were defined as those droplets with a diameter higher than 10
262 μm , as these larger areas of fat are most likely pools of free fat (Everett and Auty 2008). Fat
263 droplets with a diameter between 6-10 μm did not fit these descriptions and were excluded from
264 this analysis. In each case, the percentage of fat volume corresponding to globular or non-globular
265 fat was quantified.

266 2.7. Statistical analysis

267 The IBM-SPSS Statistics software version 24.0 (New York, NY, USA) was used for statistical
268 analysis. The general linear model of Analysis of Variance (ANOVA) was used to study the
269 effects of the two factors, CGS ($l = 2$) and CT ($l = 2$) on the composition, microstructure, texture
270 and yield variables measured in this study. The fixed effects model $Y_{ijk} = \mu + GS_i + CGS_j + CT_k$
271 $+ d\alpha y_l + (CGS*CT)_{jk} + \varepsilon_{ijkl}$ was applied to study simultaneously the effect of both factors and the
272 gel strength (GS) was used as a covariable. The relationship between texture and microstructure

273 parameters of cheese samples were studied using Pearson bivariate correlations. Statistical
 274 significance was defined as $P \leq 0.05$.

275 3. Results and discussion

276 3.1. Curd grain size and cooking temperature

277 Cheesemaking experiments were performed where the curd grain size (CGS) and cooking
 278 temperature (CT) were varied to assess the impact of these parameters. The area of the large curd
 279 grains assessed by image analysis was significantly ($P \leq 0.05$) greater than the area of the small
 280 curd grains (Table 1). As expected, this difference was significant for grains assessed both after
 281 cutting (FCG) and after cooking (SCG), indicating the effectiveness of the manual wire mesh
 282 technique and number of cuts used to alter curd grain size. Direct comparisons between the curd
 283 grain size produced here and in previous studies is made difficult by the use of different measures
 284 of curd sizes, including previous indirect measures of knife spacing and curd weight after sieving.
 285 Nevertheless the method used here provides a good span of sizes (Aldalur et al. 2019; Johnston
 286 et al. 1991; Whitehead and Harkness 1954).

287 **Table 1.** Technical parameters controlled during the experimental cheesemaking design assessing the effect of curd
 288 grain size (CGS) and cooking temperature (CT). Two replicates ($n = 2$) were carried out for each of the four treatments
 289 and the data presented is the mean \pm standard deviation.

Factors		FCG area (mm ²)	SCG area (mm ²)	Milk pH	Coagulation pH	Cutting pH	Cooking pH	Whey draining pH	Cheese pH after pressing
CT	CGS								
36°C	Big	52.53 ^a \pm 5.30	7.48 ^a \pm 0.66	6.54 \pm 0.01	6.53 \pm 0.01	6.51 \pm 0.01	6.49 \pm 0.01	6.41 \pm 0.04	5.46 \pm 0.01
45°C	Big	45.06 ^a \pm 8.35	6.46 ^a \pm 1.03	6.53 \pm 0.04	6.52 \pm 0.01	6.50 \pm 0.01	6.48 \pm 0.18	6.35 \pm 0.04	5.56 \pm 0.11
36°C	Small	14.42 ^b \pm 3.21	4.54 ^b \pm 1.41	6.56 \pm 0.04	6.52 \pm 0.00	6.51 \pm 0.04	6.38 \pm 0.04	6.41 \pm 0.04	5.41 \pm 0.01
45°C	Small	12.69 ^b \pm 4.44	3.63 ^b \pm 1.04	6.54 \pm 0.04	6.52 \pm 0.01	6.50 \pm 0.03	6.40 \pm 0.02	6.33 \pm 0.03	5.48 \pm 0.01

290 FCG, curd grain after cutting; SCG, curd grain after cooking.

291 ^{a,b} Different superscripts in the same column indicate statistically significant differences ($P \leq 0.05$).

292 3.2. Physico-chemical composition and cheese yield

293 Table 2 shows the physico-chemical parameters measured for the curd grains during cooking
 294 (SCG) and cheese from the trials described in Table 1. The significant ($P \leq 0.05$) differences
 295 observed among treatments are mainly due to an increase in dry matter content of the curd grains

296 and cheese samples when subjected to higher cooking temperatures, as temperature greatly
297 increases the rate of curd syneresis (Dejmek and Walstra 2004). Regarding the effect of curd grain
298 size, measured with varied indices, previous authors have reported a higher moisture content in
299 cheese made from bigger curd grains (Johnston et al. 1991; Whitehead and Harkness 1954). In
300 other studies, however, the effect of curd grain size was reported have no impact on the dry matter
301 content of the cheese (Everard et al. 2008). In this study, no significant difference ($P > 0.05$) was
302 observed for the dry matter of the cheese samples using both big and small curd grain sizes,
303 consistent with the results obtained by Everard et al. (2008).

304 The fat in dry matter content in the cheese samples was significantly ($P \leq 0.05$) affected by the
305 curd grain size, indicating that the bigger particles retained more fat (Table 2). Similarly, the fat
306 loss was also higher when the curd grain was smaller (Table 3). Reducing the curd grain size
307 increases the surface area to volume ratio and the loss of fat globules to the whey is consequently
308 enhanced (Banks 2007). This process could be visualised using confocal microscopy, as shown
309 in [Online Resource 2](#), where the fat globules near the edge of the curd grain are observed readily
310 entering the surrounding solution after the protein matrix of the curd is cut and this process is
311 likely responsible for the differences in fat loss observed with different sized curd. No visual
312 differences were observed, however, between the edges of the curd with difference grain sizes.

313
314

Table 2. General composition (mean \pm standard deviation) of curd grains after cooking and cheese samples from the experimental cheesemaking design combining the factors curd grain size (*CGS*) and cooking temperature (*CT*).

	Big <i>CGS</i>		Small <i>CGS</i>		Significance		
	36 °C	45 °C	36 °C	45 °C	<i>CGS</i>	<i>CT</i>	<i>CGS*CT</i>
Curd grains after cooking							
Fat, g/100 g	17.1 \pm 1.6	24.0 \pm 0.7	17.5 \pm 1.1	22.5 \pm 0.4	ns	**	ns
Fat in dry matter, g/100 g	42.0 \pm 1.7	48.0 \pm 2.7	44.9 \pm 1.5	47.4 \pm 1.3	ns	ns	ns
Protein, g/100 g	16.10 \pm 1.97	20.50 \pm 1.85	14.24 \pm 0.24	20.41 \pm 0.18	ns	**	ns
Protein in dry matter, g/100 g	39.45 \pm 2.72	40.92 \pm 2.61	36.55 \pm 1.61	43.02 \pm 0.89	ns	ns	ns
Dry Matter, g/100 g	40.74 \pm 2.17	50.07 \pm 1.31	38.97 \pm 1.07	47.44 \pm 0.57	*	***	ns
Calcium, mg/100 g	661 \pm 50	842 \pm 11	623 \pm 55	874 \pm 35	ns	**	ns
Phosphorous, mg/100 g	426 \pm 27	527 \pm 53	399 \pm 32	545 \pm 23	ns	**	ns
Magnesium, mg/100 g	42 \pm 3	52 \pm 1	40 \pm 4	53 \pm 2	ns	**	ns
Cheese							
Fat, g/100 g	28.5 \pm 0.0	30.0 \pm 0.7	27.9 \pm 0.2	29.0 \pm 0.0	ns	*	ns
Fat in dry matter, g/100 g	52.8 \pm 0.4	52.6 \pm 0.8	51.4 \pm 0.6	50.1 \pm 0.3	*	ns	ns
Protein, g/100 g	21.90 \pm 0.07	24.00 \pm 0.26	23.12 \pm 0.33	24.27 \pm 0.16	*	**	*
Protein in dry matter, g/100 g	40.52 \pm 0.44	42.10 \pm 0.82	42.66 \pm 1.36	41.91 \pm 0.54	ns	ns	ns
Dry Matter, g/100 g	54.04 \pm 0.40	57.02 \pm 0.49	54.22 \pm 0.96	57.91 \pm 0.36	ns	**	ns
Calcium, mg/100 g	986 \pm 28	1062 \pm 34	990 \pm 1	1104 \pm 21	ns	**	ns
Phosphorous, mg/100 g	596 \pm 4	648 \pm 21	610 \pm 2	675 \pm 8	ns	**	ns
Magnesium, mg/100 g	56 \pm 1	61 \pm 2	59 \pm 1	65 \pm 6	*	**	ns

315

*, $P \leq 0.05$; **, $P \leq 0.01$; ***, $P \leq 0.001$; ns, not significant where $P > 0.05$.

316 The fat content in the whey obtained in this study was also higher than in previous studies (0.79
317 ± 0.13 vs $0.30-0.48$ g/100 g in previous studies). The difference in fat content could be due to
318 several factors such as a higher milk fat concentration (6.14 ± 0.17 vs $2.9-5.1$ g/100g in previous
319 studies), the use of ovine milk rather than bovine milk, a higher stirring speed (40 rpm in a 20 L
320 capacity vat vs 10 to 22 rpm in 11 L vats or 4 to 7 rpm in over 20,000 L vats), differences in the
321 cheesemaking processing conditions, or the method of manual cutting and use of nylon wires for
322 cutting the curd (Everard et al. 2008; Johnston et al. 1991; Johnston et al. 1998). Such wires can
323 break the gel, producing curd grains with coarse surfaces causing a high number of mini curd
324 particles, increasing fat losses in the whey (Kammerlehner 2009). There was some evidence of
325 such small particles in all treatments here observed by CLSM, where the curd junction could be
326 seen to surround the curd particle, where particles were typically $\sim 200-400$ μm in diameter
327 ([Online Resource 3](#)). Similar consistent observations were made by cryo-SEM.

328 The total number of revolutions has also been shown previously to influence fat losses. Several
329 authors have shown using cow milk that when the total revolutions of the cutting process are
330 insufficient, the subsequent stirring leads to the shattering of curd particles and increases the
331 amount of fat in the whey, whereas fat losses can be contained when the number of revolutions
332 during cutting is increased (Everard et al. 2008; Johnston et al. 1991; Johnston et al. 1998). In a
333 recent study using raw sheep milk, a higher number of stirring revolutions also caused higher fat
334 losses in the whey (Aldalur et al. 2019). In the present study, the number of total revolutions (or
335 equivalent number of cuts) appears higher than the above cited studies, suggesting that greater
336 curd cutting and stirring has the potential to also be damaging.

337 The protein content, unlike the fat, appeared less affected by the curd grain size and cooking
338 temperature. While differences were observed for selected conditions (a smaller *CGS* and higher
339 *CT* and the interaction term *CGS*CT* indicated higher protein) these were not significant once
340 corrected for moisture and compared on the basis of protein in dry matter.

341 The cooking temperature was the main factor affecting the mineral composition of the cheese and
 342 the curd grain size had no significant effect (Table 2). The calcium, phosphorous and magnesium
 343 contents were significantly ($P \leq 0.05$) higher in cheeses cooked at the higher temperature of 45
 344 °C. Consequently, the calcium in the whey was also significantly ($P \leq 0.05$) higher when the
 345 cooking temperature was lower at 36 °C (Table 3). Interestingly, these differences occurred
 346 despite the similar pH at whey draining (Table 1); another factor known to influence calcium loss
 347 during cheesemaking (Johnson and Lucey 2006).

348 **Table 3.** Actual yield, moisture-adjusted yield, yield efficiency and component losses (mean \pm standard deviation)
 349 obtained from the experiments assessing the effect of curd grain size (*CGS*) and cooking temperature (*CT*).

	Big <i>CGS</i>		Small <i>CGS</i>		Significance		
	36 °C	45 °C	36 °C	45 °C	<i>CGS</i>	<i>CT</i>	<i>CGS*CT</i>
Fat loss (%)	8.60 \pm 0.78	9.11 \pm 1.46	10.81 \pm 0.23	11.35 \pm 0.06	*	ns	ns
Protein loss (%)	22.39 \pm 0.66	23.82 \pm 4.44	22.91 \pm 1.01	22.76 \pm 0.50	ns	ns	ns
Calcium loss (%)	23.67 \pm 4.87	19.83 \pm 1.63	22.17 \pm 3.37	20.05 \pm 0.86	ns	*	ns
Phosphorous loss (%)	36.98 \pm 1.71	36.71 \pm 2.07	37.23 \pm 2.02	36.87 \pm 3.38	ns	ns	ns
Magnesium loss (%)	60.20 \pm 0.48	60.90 \pm 1.17	61.14 \pm 1.52	62.50 \pm 0.59	ns	ns	ns
Actual yield (kg/100 kg)	19.21 \pm 0.74	18.43 \pm 0.37	19.16 \pm 0.24	17.96 \pm 0.48	**	***	**
Moisture-adjusted yield (kg/100 kg)	18.87 \pm 0.58	19.10 \pm 0.22	18.89 \pm 0.09	18.91 \pm 0.38	ns	ns	ns
Yield efficiency (%)	97.09 \pm 0.63	98.29 \pm 2.57	97.23 \pm 4.13	97.28 \pm 1.67	ns	ns	ns

350 *, $P \leq 0.05$; **, $P \leq 0.01$; ***, $P \leq 0.001$; ns, not significant where $P > 0.05$.

351 The actual yield (Y_A) was statistically affected by both, the curd grain size and cooking
 352 temperature ($P \leq 0.05$; Table 3). The yield increased when the curd grain size was bigger and the
 353 cooking temperature was lower. The interaction term *CGS*CT* was also statistically significant
 354 ($P \leq 0.05$), indicating that both factors had an impact on the cheese yield. These differences were
 355 mainly associated with the dry matter content of the cheese samples, however, as once corrected
 356 for moisture the moisture adjusted yield (Y_{MA}) was not significantly different for these treatments
 357 ($P > 0.05$; Table 3). The relationship between cheese yield and dry matter has been well
 358 documented by other authors (Lucey and Kelly 1994; Whitehead and Harkness 1954). The
 359 moisture-adjusted yield was expected to be different due to an increased amount of fat loss in the
 360 whey observed for small curd grains (Table 3), however, this loss appears to be insignificant
 361 compared to the weight of the cheese samples. Consequently, we consider the amount of fat loss

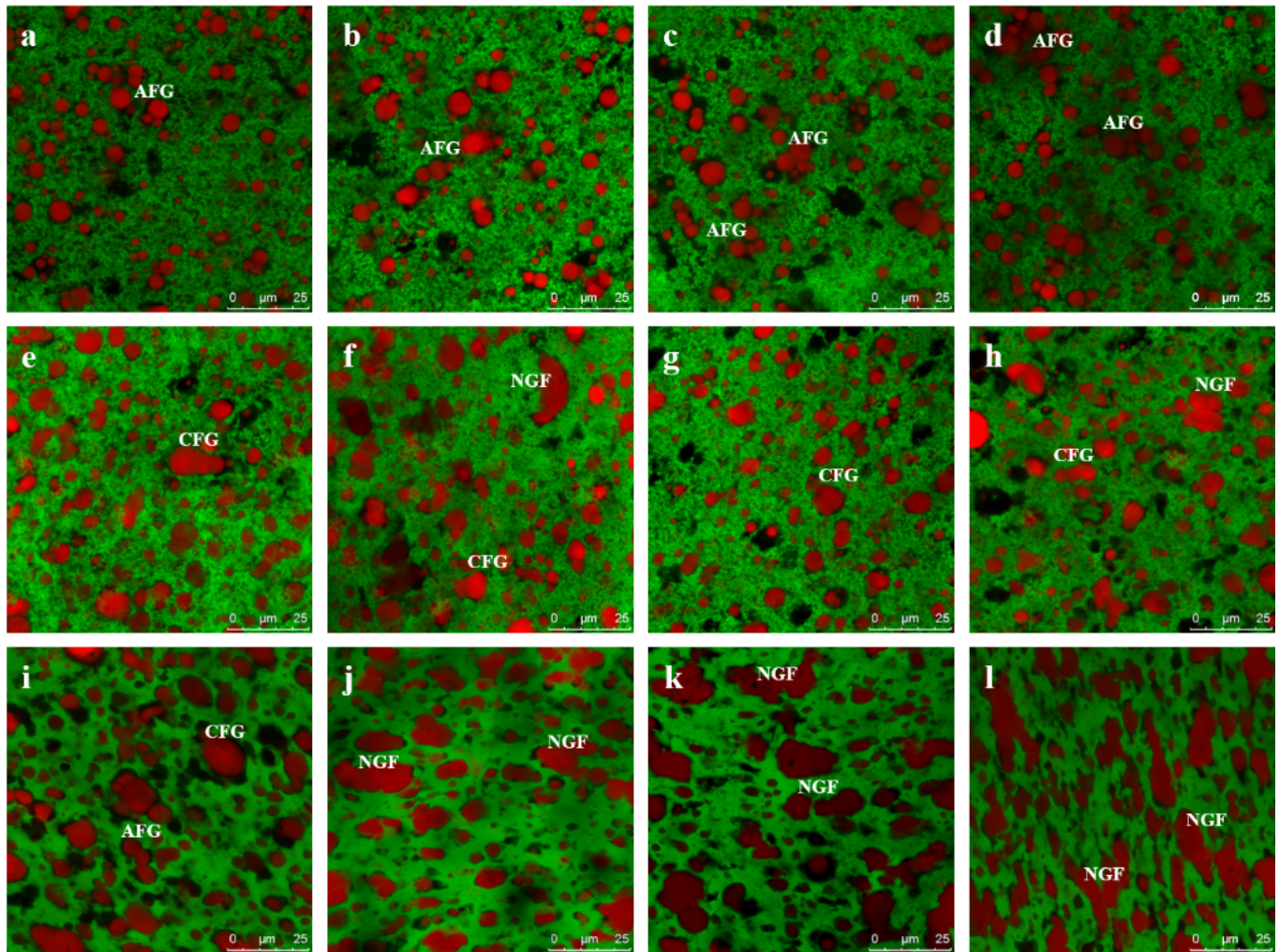
362 a better indicator of cheese yield when observing small differences between temperatures and
363 curd grain sizes in cheesemaking. Other studies have similarly observed fat loss to be a more
364 sensitive measure when operating a small pilot scale (Ong et al. 2015). The high fat losses in this
365 study were also reflected in the low cheese yield efficiency (Table 3), as the average values for
366 Y_{MA} were below the calculated theoretical cheese yield (19.44 ± 0.55 kg/100 kg). This again may
367 be due to several factors including the composition of milk, the method of cutting, number of total
368 revolutions and pilot scale of the study.

369 3.3. *Microstructure of curd and cheese*

370 Changes in the microstructure of dairy matrices were followed by confocal microscopy during
371 the cheesemaking process to visualise the effects of *CGS* and *CT*. The rennet-induced gel had a
372 compact structure for all cheesemaking treatments, with a mean porosity of 0.36 ± 0.08 . This low
373 porosity was expected, due to the high fat and protein content of raw sheep milk ([Online Resource](#)
374 [4](#); [Online Resource 1](#)). In comparison, Ong et al. (2010) reported 0.49 ± 0.02 porosity for gels
375 formed from raw cow's milk where the fat and protein content were lower with a concentration
376 of 4.45 g/100 g and 3.53 g/100 g, respectively.

377 Fat droplets were numerous in rennet-induced gel samples. The mean diameter determined by
378 image analysis was 7.25 ± 0.74 μm , which was not significantly ($P > 0.05$) different to the mean
379 diameter of milk samples determined using the same method (5.93 ± 0.48 μm). In agreement with
380 other studies, the fat droplets appear to act as inner fillers, as the casein network was formed
381 around the fat globules with no visible interaction between the protein and fat components (Lopez
382 et al. 2007; Michalski et al. 2002). Some fat globules formed aggregates or coalesced droplets but
383 generally the globular structure of fat was retained throughout this stage of the cheesemaking
384 process ([Online Resource 4](#)).

385 The protein matrix contracted during the cheesemaking process (Fig. 1), as the dry matter content
386 significantly ($P \leq 0.05$) increased due to the syneresis (Table 2). The size of the fat globules was
387 similar to within the gel after cutting (7.58 ± 0.86 μm) but these droplets began to change in shape

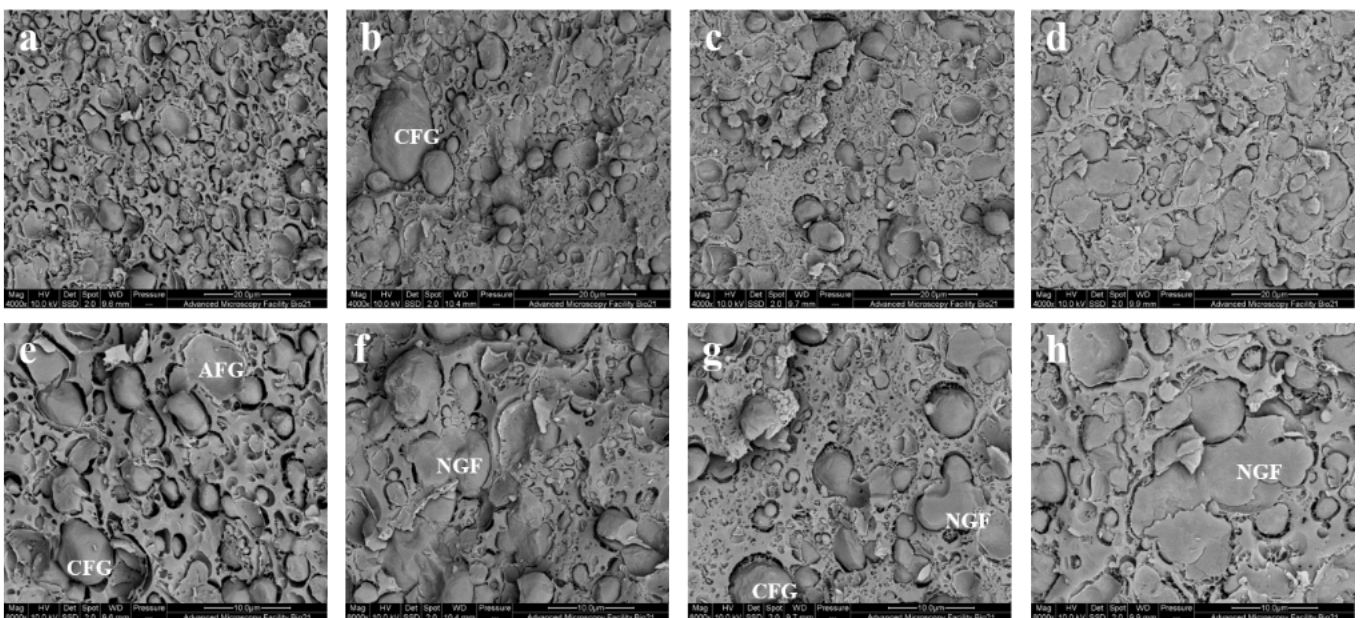


388 **Fig. 1:** Confocal laser scanning microscopy images of (a to d) curd grains after cutting, (e to h) curd grains after cooking
 389 and (i to l) cheese, of the combination of factors curd grain size (*CGS*) and cooking temperature (*CT*) during the
 390 cheesemaking process. Cheesemaking treatments were coded as: big *CGS* and 36 °C *CT* (a, e, i); big *CGS* and 45 °C
 391 *CT* (b, f, j); small *CGS* and 36 °C *CT* (c, g, k); small *CGS* and 45 °C *CT* (d, h, l). Images were obtained using a 63x
 392 objective lens and digitally magnified 2x. Fat appears red and protein appears green in these images. The scale bars are
 393 25 μm in length. AFG = aggregates of fat globule, CFG = coalesced fat globule, NGF = non-globular fat.

394 following cooking and pressing (Fig. 1, e to l). Some fat globules fused together during cooking
 395 generating coalesced fat globules, whilst some non-globular or free fat could also be observed
 396 (Fig. 1, f and j). After pressing, the fat volume significantly increased ($P \leq 0.05$) and the structure
 397 of nearly all fat globules was disrupted (Fig. 1, i to l).

398 The cooking temperature was found to significantly affect the physical properties of the cheese
 399 measured by 3D image analysis of the CLSM micrographs. When the cooking temperature
 400 increased to 45 °C, the volume of non-globular fat increased significantly ($P \leq 0.05$) in cheese
 401 samples (Table 4). This was observed by both CLSM (Fig. 1; j and l) and cryo-SEM imaging

402 (Fig. 2; b, d, f and h). Most of the fat droplets in these micrographs appeared to have lost their
 403 globular structure and the fat appeared as coalesced non-globular fat. Conversely, the volume
 404 contributed by globular fat significantly decreased ($P \leq 0.05$) when the stirring temperature was
 405 45 °C; few globular fat droplets were also observed when the curd grain size was smaller (Table
 406 4), indicating that these smaller fat globules fused to form larger coalesced fat globules and free
 407 fat (Lopez et al. 2006). Additionally, a smaller curd grain size can lead to a higher compaction of
 408 the curd during pressing (Walstra et al. 2006); this could cause further disruption of the fat
 409 droplets, resulting in more non-globular fat as detected by image analysis here.



410 **Fig. 2:** Cryo-scanning electron microscopy images of cheese of the combination of factors curd grain size (*CGS*) and
 411 cooking temperature (*CT*) during the cheesemaking. Cheesemaking treatments were coded as: big *CGS* and 36 °C *CT*
 412 (a, e); big *CGS* and 45 °C *CT* (b, f); small *CGS* and 36 °C *CT* (c, g); small *CGS* and 45 °C *CT* (d, h). Representative
 413 images were presented at 4000x magnification (a to d) and 8000x magnification (e to h). The scale bars are 20 µm (A)
 414 and 10 µm (B) in length. AFG = aggregates of fat globule, CFG = coalesced fat globule, NGF = non-globular fat.

415 The effect of temperature on the cheese matrix structure could be also observed by analysing the
 416 porosity (Table 4), as the curd grains heated at 36 °C or 45 °C had porosities of 0.17 ± 0.03 and
 417 0.10 ± 0.03 , respectively, with the higher temperature reducing network porosity ($P \leq 0.05$). This
 418 effect of temperature could also be observed visually by cryo SEM, as gaps could be seen at the
 419 interface between the fat and protein network of the cheese cooked at 36 °C with big curd granules
 420 (Fig. 2e).

421 The surface of the curd grains contained little fat content once the curd was pressed and the curd
422 junctions were evident as thick protein strands within the cheese microstructure ([Online Resource](#)
423 [5](#)). Several calcium phosphate crystalline inclusions were also observed (white arrows in [Online](#)
424 [Resource 5](#)) and these generally occurred along the curd junction in all four treatments, as calcium
425 in dry matter basis was not significantly different ($P > 0.05$) in these cheese samples ([Online](#)
426 [Resource 6](#)). This structural arrangement has also been reported in other cheeses (Brooker et al.
427 1975; D’Incecco et al. 2016; Ong et al. 2015), with the number of inclusions increasing after
428 calcium addition. D’Incecco et al. (2016) attributed the increased number of crystalline inclusions
429 within the curd junction to be a result of incomplete aggregation of the curd granules and the
430 higher volume of whey initially present within the curd junctions. The resulting dense spherulite
431 crystals likely arise from non-crystalline branching from a nuclei core. These nuclei could form
432 from the supersaturated concentration of solutes originating in the whey; a condition that is known
433 to lead to spherulite formation in gels (Shtukenberg et al. 2011), such as the protein network
434 observed here.

435 *3.4. Cheese texture*

436 Cooking temperature was the main factor found to affect the textural parameters of the cheese
437 (Table 4). A higher cooking temperature (45 °C) produced cheeses that were significantly ($P \leq$
438 0.05) harder and chewier than those produced at lower temperatures (36 °C). Cheese texture is
439 known to be affected by many factors such as the composition, microstructure, fat droplet size
440 and distribution, casein matrix bond strength and interactions between fat globules and the protein
441 matrix (Everett and Auty 2008; Hickey et al. 2015). Here, the differences observed with higher
442 temperature were likely due to the higher fat, protein, mineral and dry matter content in the
443 cheeses cooked at 45 °C (Table 2). Conversely, the curd granule size was not found to significantly
444 impact ($P > 0.05$) on the cheese textural parameters.

445 **Table 4.** Physical properties obtained by 3D image analysis and texture parameters (mean \pm standard deviation) of
 446 cheese samples from experiments assessing the effect of curd grain size (*CGS*) and cooking temperature (*CT*).

Physical properties	Big <i>CGS</i>		Small <i>CGS</i>		Significance		
	36°C	45°C	36°C	45°C	<i>CGS</i>	<i>CT</i>	<i>CGS*CT</i>
Fat sphericity	0.60 \pm 0.00	0.58 \pm 0.02	0.61 \pm 0.04	0.56 \pm 0.05	ns	ns	ns
Porosity	0.18 \pm 0.05	0.11 \pm 0.00	0.17 \pm 0.01	0.09 \pm 0.05	ns	*	ns
Volume of globular fat (%)	12 \pm 1	4 \pm 2	7 \pm 2	3 \pm 2	*	**	ns
Volume of non-globular fat (%)	69 \pm 6	92 \pm 0	78 \pm 11	96 \pm 2	ns	*	ns
Cheese texture							
Hardness (g)	5389 \pm 518	7796 \pm 649	6653 \pm 1307	8414 \pm 296	ns	*	ns
Chewiness (g)	2989 \pm 560	4834 \pm 308	3845 \pm 1086	5284 \pm 403	ns	*	ns
Springiness (s/s)	0.846 \pm 0.002	0.858 \pm 0.004	0.858 \pm 0.007	0.865 \pm 0.011	ns	ns	ns
Cohesiveness (g·s/g·s)	0.654 \pm 0.056	0.716 \pm 0.004	0.669 \pm 0.065	0.726 \pm 0.022	ns	ns	ns
Resilience (g·s/g·s)	0.338 \pm 0.029	0.373 \pm 0.000	0.360 \pm 0.026	0.391 \pm 0.020	ns	ns	ns

447 *, $P \leq 0.05$; **, $P \leq 0.01$; ns, not significant where $P > 0.05$.

448 In addition, the textural parameters measured were correlated with the microstructural properties
 449 of cheese quantified by 3D image analysis. The cheeses in which a higher volume of globular fat
 450 was retained (i.e. cheese cooked at 36 °C and or using a larger curd grain size) had lower hardness,
 451 chewiness, cohesiveness and resilience ($r > |0.7|$, $P \leq 0.05$), while those cheeses with a higher
 452 volume of non-globular fat (i.e. cheese cooked at 45 °C) had higher values in textural parameters
 453 ($r > 0.7$, $P \leq 0.05$; i.e. were harder, chewier and had greater cohesiveness and resilience). Fat is
 454 known to act as an inert filler when the globular structure is maintained, retaining a softer cheese
 455 texture (Everett and Auty 2008), as was observed here. Cheese springiness also showed an
 456 interesting negative correlation with the porosity of the protein network ($r = |0.7|$; $P \leq 0.05$), with
 457 more porous cheeses demonstrating a reduced ability to spring back on compression; this may be
 458 due to the higher number of cavities and network imperfections observed in the most porous
 459 cheese structures (e.g. Fig. 2e).

460 **4. Conclusions**

461 This study indicates that curd grain size and cooking temperature affect the structural and textural
 462 characteristics of cheese made using raw sheep milk, in addition to affecting the yield and
 463 composition of the whey generated during the cheesemaking process. The cooking temperature

464 had a major effect on cheese composition, increasing the dry matter content of the cheese due to
465 the enhanced syneresis during cooking. A higher cooking temperature significantly altered the
466 texture of the cheese, increasing hardness and chewiness. Additionally, changes in the
467 microstructure were observed with different cooking temperatures, with high temperatures
468 increasing non-globular fat and reducing the porosity of the cheese protein matrix. These changes
469 of the structural arrangement of fat were correlated with the textural properties of cheese. A small
470 curd grain size was the main factor responsible for increased fat losses in the whey. Consequently,
471 the actual cheese yield was impaired when the cutting process was more intense and cooking
472 temperatures higher. These results contribute with new data on the interactions between curd grain
473 size and cooking conditions on the microstructural, textural and chemical properties of cheese.
474 These insights are useful for the dairy sector in order to improve and control the cheesemaking
475 process and the composition of the whey generated for ulterior processing.

476 **5. Acknowledgements**

477 The authors thank Meredith Dairy for supplying the milk used in this study. Financial support
478 was provided by The University of the Basque Country (PA16/04) and The Basque Government
479 (IT944-16). A. Aldalur thanks The Basque Government for the research fellowship. The research
480 was supported by The Australian Research Council (ARC) Industrial Transformation Research
481 Program (ITRP) funding scheme (Project Number: IH120100005). The ARC Dairy Innovation
482 Hub is a collaboration between The University of Melbourne, The University of Queensland and
483 Dairy Innovation Australia Ltd. We thank The Biological Optical Microscopy Platform at The
484 Bio21 Molecular Science & Biotechnology Institute for equipment access.

485 **References**

- 486 Aldalur, A., Bustamante, M.A., & Barron, L.J.R. (2019). Characterization of curd grain size and
487 shape by two-dimensional image analysis during the cheesemaking process in artisanal sheep
488 dairies. *Journal of Dairy Science*, 102, 1083-1095.
- 489 AOAC (2005) Fat in raw milk, Babcock method, Method N° 989.04. In W. Horowitz (Ed.) 18th
490 edition, *Official Methods of Analysis of AOAC International* (pp. 23-25). Gaithersburg, MD:
491 AOAC International.
- 492 Banks J.M. (2007). Cheese yield. In P.L.H. McSweeney (Ed.), *Cheese problems solved* (pp. 100-
493 114). Cambridge, England: Woodhead Publishing Limited.
- 494 Barbano, D.M., & Sherbon, J.W. (1984). Cheddar cheese yields in New York. *Journal of Dairy*
495 *Science*, 67, 1873-1883.
- 496 Brooker, B.E., Hobbs, D.G., & Turvey, A. (1975). Observations on the microscopic crystalline
497 inclusions in Cheddar cheese. *Journal of Dairy Research*, 42, 341-348.
- 498 Chen, G.Q., Eschbach, F.I.I., Weeks, M., Gras, S.L., & Kentish, S.E. (2016). Removal of lactic
499 acid whey using electrodialysis. *Separation and Purification Technology*, 158, 230-237.
- 500 Dejmek, P., & Walstra, P. (2004). The syneresis of rennet-coagulated curd. In P. F. Fox, T. P.
501 Guinee, T. M., Cogan, & P. L. H., McSweeney (Eds.), *Cheese: Chemistry, Physics and*
502 *Microbiology. Volume 1. General Aspects* (pp. 71–103). London, UK: Elsevier Applied Science.
- 503 D’Incecco, P., Limbo, S., Faoro, F., Hogenboom, J., Rosi, V., Morandi, S., Pellegrino, L. (2016).
504 New insight on crystal and spot development in hard and extra-hard cheeses: Association of spots
505 with incomplete aggregation of curd granules. *Journal of Dairy Science*, 99, 1-13.
- 506 El-Bakry, M. & Sheehan, J. (2014). Analysing cheese microstructure: A review of recent
507 developments. *Journal of Food Engineering*, 125, 84-96.

508 Emmons, D.B. & Modler, H.W. (2010). Invited review: A commentary on predictive cheese yield
509 formulas. *Journal of Dairy Science*, *93*, 5517-5537.

510 EUROSTAT. Agriculture, forestry and fishery statistics - Milk and milk product statistics. (2016).
511 European Commission, Luxembourg. [https://ec.europa.eu/eurostat/statistics-
512 explained/index.php/Milk_and_milk_product_statistics#undefined](https://ec.europa.eu/eurostat/statistics-explained/index.php/Milk_and_milk_product_statistics#undefined) Accessed October 1, 2018.

513 Everard, C. D., O'Callaghan, D. J., Mateo, M. J., O'Donnell, C. P., Castillo, M., & Payne, F. A.
514 (2008). Effects of Cutting Intensity and Stirring Speed on Syneresis and Curd Losses During
515 Cheese Manufacture. *Journal of Dairy Science*, *91*, 2575–2582.

516 Everett, D.W., & Auty M.A.E. (2008). Cheese structure and current methods of analysis.
517 *International Dairy Journal*, *18*, 759-773.

518 Fagan, C.C., Castillo, M., Payne, F.A., O'Donnell, C.P., & O'Callaghan, D.J. (2007). Effect of
519 cutting time, temperature, and calcium on curd moisture, whey fat losses and curd yield by
520 response surface methodology. *Journal of Dairy Science*, *90*, 4499-4512.

521 Guinee, T. P., O'Kennedy, B. T., & Kelly P. M. (2006). Effect of milk protein standardization
522 using different methods on the composition and yields of Cheddar cheese. *Journal of Dairy
523 Science*, *89*, 468-482.

524 Gunasekaran, S. & Ding, K. (1998). Three-dimensional characteristics of fat globules in Cheddar
525 cheese. *Journal of Dairy Science*, *82*, 1890-1896.

526 Hickey, C.D., Auty, M.A.E., Wilkinson, M.G., & Sheehan, J.J. (2015). The influence of cheese
527 manufacture parameters on cheese microstructure, microbial localisation and their interactions
528 during ripening: A review. *Trends in Food Science & Technology*, *41*, 135-148.

529 ISO/IDF (2002). Milk and milk products – Routine method using combustion according to the
530 Dumas principle. *ISO 14891:2002/ IDF 185:2002*. Geneva, Switzerland: International
531 Standardisation Organisation.

532 ISO/IDF (2004). Cheese and processed cheese - Determination of the total solids content. *ISO*
533 *5534:2004/ IDF 4: 2004*. Geneva, Switzerland: International Standardisation Organisation.

534 ISO/IDF (2010). Milk, cream and evaporated milk – Determination of the total solids content.
535 *ISO 6731:2010/ IDF 21:2010*. Geneva, Switzerland: International Standardisation Organisation.

536 ISO/IDF (2014). Milk and milk products – Determination of nitrogen content – Part 1: Kjeldhal
537 principle and crude protein calculation. *ISO 8968-1:2014/ IDF 20-1:2014*. Geneva, Switzerland:
538 International Standardisation Organisation.

539 Johnson, M.E. & Lucey, J.A. (2006). Calcium: a key factor in controlling cheese functionality.
540 *Australian Journal of Dairy Technology*, *61*, 147-153.

541 Johnston, K. A., Dunlop, F. P., & Lawson, M. F. (1991). Effects of speed and duration of cutting
542 in mechanized Cheddar cheese. *Journal of Dairy Research*, *58*, 345–354.

543 Johnston, K. A., Luckman, M. S., Lilley, H. G., & Smale, B. M. (1998). Effect of Various Cutting
544 and Stirring Conditions on Curd Particle Size and Losses of Fat to the Whey during Cheddar
545 Cheese Manufacture in Ost Vats. *International Dairy Journal*, *8*, 281-288.

546 Kammerlehner, J. (2009). Rennet cheese (Cow's milk cheese). In Kammerlehner, J. (Ed), *Cheese*
547 *Technology* (pp. 43-624). Freising, Germany: Josef Kammerlehner.

548 Lamichhane, P., Kelly, A.L., & Sheehan, J.J. (2018). Invited review: Structure-function
549 relationships in cheese. *Journal of Dairy Science*, *101*, 1-18.

550 Logan, A., Day, L., Pin, A., Auldist, M., Leis, A., Puvanenthiran, A., & Augustin, M.A. (2014).
551 Interactive effects of milk fat globule and casein micelle size on the renneting properties of milk.
552 *Food Bioprocess Technology*, *7*, 3175-3185.

553 Lopez C., Briard-Bion, V., Camier, B., & Gassi, J.-Y. (2006). Milk fat thermal properties and
554 solid fat content in Emmental cheese: a differential scanning calorimetry study. *Journal of Dairy*
555 *Science*, *89*, 2894-2910.

556 Lopez, C., Camier, B., & Gassi, J.-Y. (2007). Development of the milk fat microstructure during
557 the manufacture and ripening of Emmental cheese observed by confocal laser scanning
558 microscopy. *International Dairy Journal*, 17, 235-247.

559 Lucey, J., & Kelly, J. (1994). Cheese yield. *Journal of the Society of Dairy Technology*, 47, 1-14.

560 Michalski, M.C., Cariou, R., Michel, F., & Garnier, C. (2002). Native vs. Damaged milk fat
561 globules: membrane properties affect the viscoelasticity of milk gels. *Journal of Dairy Science*,
562 85, 2451-2461.

563 Ong, L., Dagastine, R.R., Kentish, S.E., & Gras, S.L. (2010). The effect of milk processing on
564 the microstructure of the milk fat globule and rennet-induced gel observed using confocal laser
565 scanning microscopy. *Journal of Food Science*, 75, E135-E145.

566 Ong, L., Dagastine, R.R., Kentish, S.E., & Gras, S.L. (2011). Microstructure of milk gel and
567 cheese curd observed using cryo scanning electron microscopy and confocal microscopy. *LWT –*
568 *Food Science and Technology*, 44, 1291-1304.

569 Ong, L., Dagastine, R.R., Kentish, S.E., & Gras, S.L. (2012). The effect of pH at renneting on the
570 microstructure, composition and texture of Cheddar cheese. *Food Research International*, 48,
571 119-130.

572 Ong, L., Soodam, K., Kentish, S.E., Powell, I.B., & Gras, S.L. (2015). The addition of calcium
573 chloride in combination with a lower draining pH to change the microstructure and improve fat
574 retention in Cheddar cheese. *International Dairy Journal*, 46, 53-62.

575 Park, Y.W., Juárez, M., Ramos, M., & Haenlein, G.F.W. (2007). Physico-chemical characteristics
576 of goat and sheep milk. *Small Ruminant Research*, 68, 88-113.

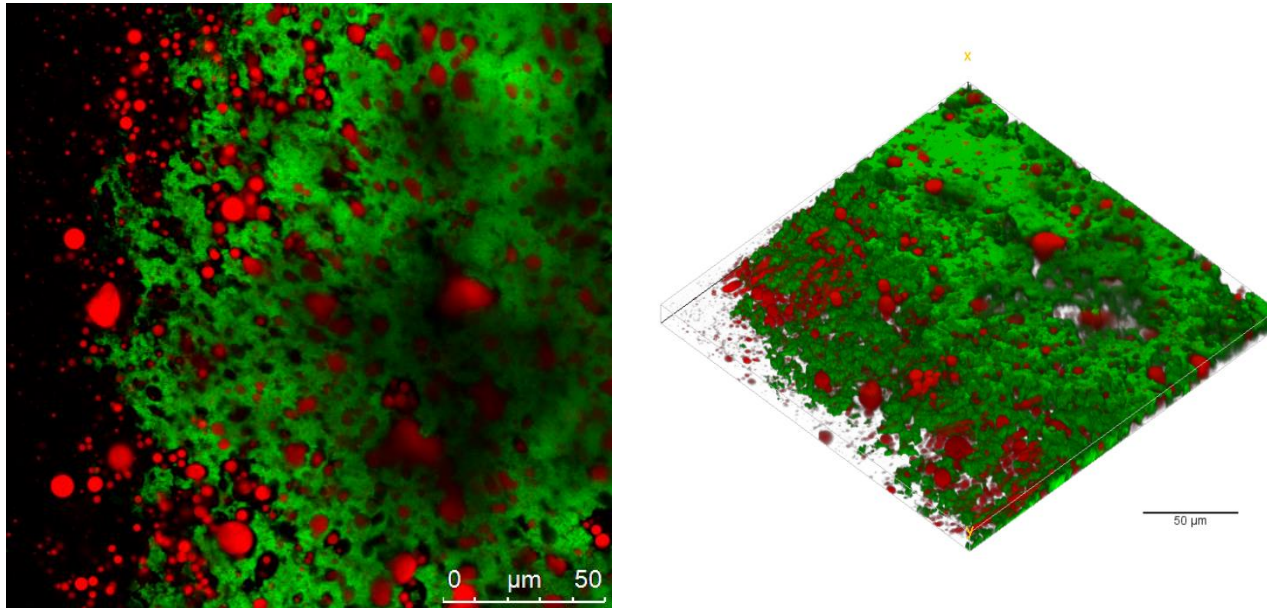
577 Ridler, T.W., & Calvard, S. (1978). Picture thresholding using an iterative selection method. *IEEE*
578 *Transactions on Systems, Man and Cybernetics*, 8, 630-632.

- 579 Shtukenberg, A.G., Punin, Y.O., Gunn, E., & Kahr, B. (2011). Spherulites. *Chemical Reviews*,
580 112, 1805-1838.
- 581 Walstra, P., Wouters, J.T.M., & Geurts, T.J. (2006). Cheese Manufacture. In P., Walstra, J.T.M.,
582 Wouters, T.J., Geurts (Eds). *Dairy Science and Technology. Second Edition* (pp. 583-639). Boca
583 Raton, FL, US. CRC Press.
- 584 Whitehead, H. R., & Harkness, W. L. (1954). The influence of variations in cheese-making
585 procedure on the expulsion of moisture from Cheddar cheese curd. *The Australian Journal of*
586 *Dairy Technology*, 9, 103–107.

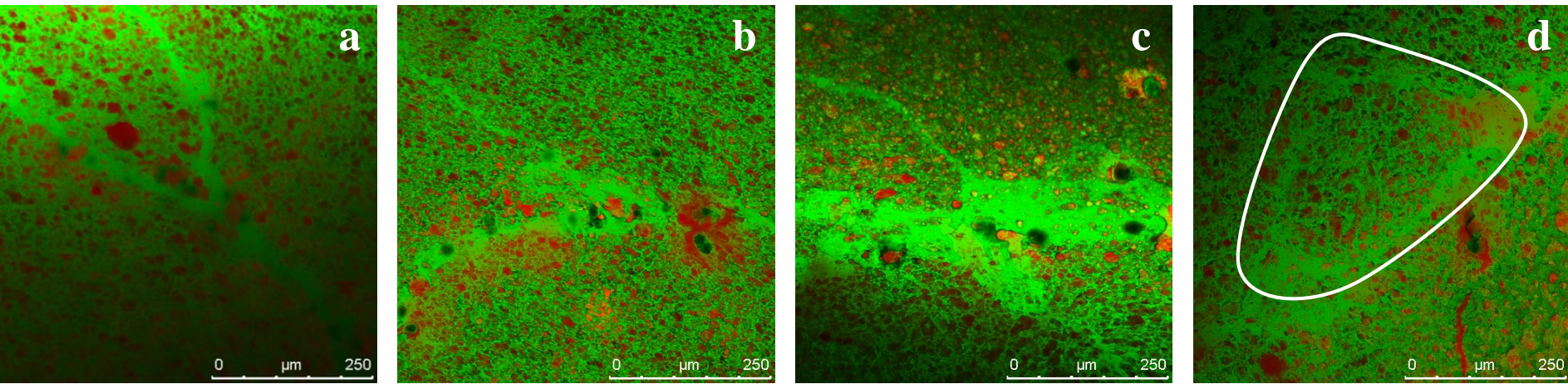
Online Resource 1. Chemical composition, rheological properties and fat globule size (mean \pm standard deviation) of the raw ewe's milk used for experimental cheesemaking. Bulk milk was collected from a commercial farm on two consecutive weeks (n = 2).

Fat, g/100 g	6.14 \pm 0.17
Protein, g/100 g	5.25 \pm 0.14
Dry matter, g/100 g	17.91 \pm 0.38
Calcium, mg/100 mL	158 \pm 8
Magnesium, mg/100 mL	16 \pm 1
Phosphorous, mg/100 mL	134 \pm 14
Fat globule size D[4,3], μm^1	4.29 \pm 0.12
Onset gelation, s	882 \pm 55
Curd firming rate, Pa/s	0.16 \pm 0.03
Final curd firmness, Pa	320 \pm 42

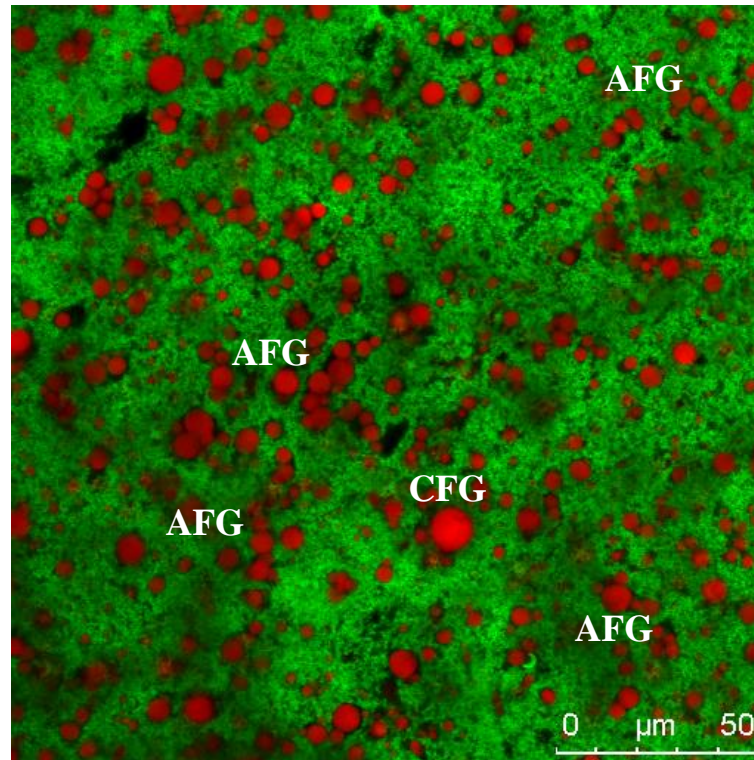
¹Measured by light scattering.



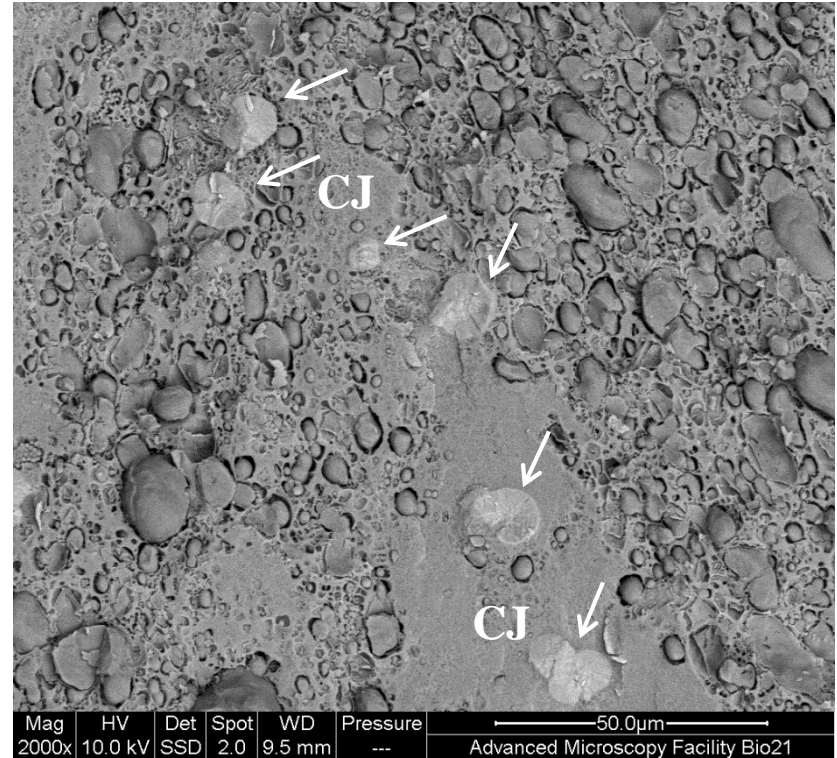
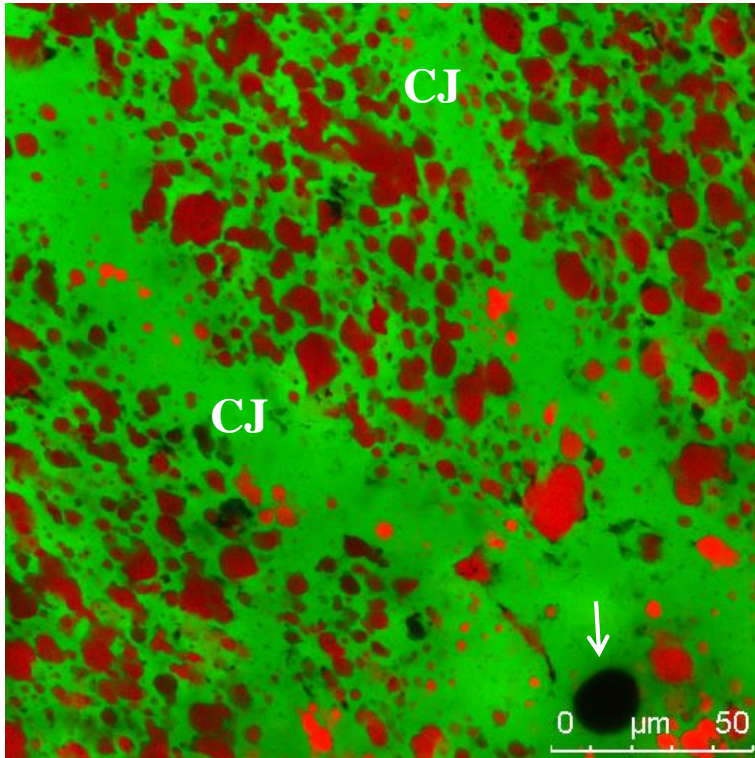
Online Resource 2: Confocal laser scanning microscopy micrograph in 2-D (left) and 3-D reconstruction (right) showing the release of fat globules from the curd grain (small size) after cooking (45 °C). Images were acquired using a 63x objective lens. Fat appears red and protein appears green in this image. The scale bar is 50 μm in length.



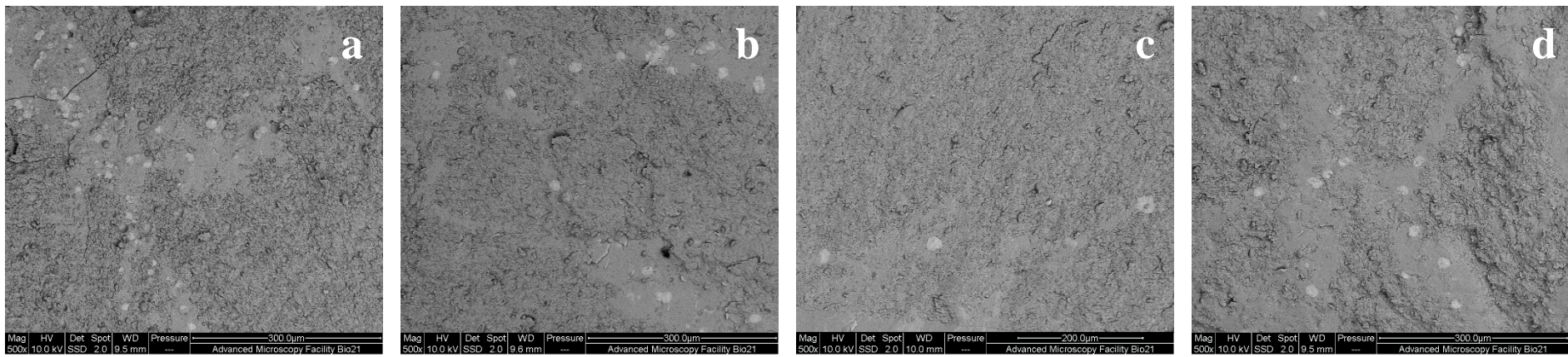
Online Resource 3: Confocal laser scanning microscopy images showing mini curd particles and curd junctions in cheese samples. Cheesemaking treatments were coded as: big CGS and 36 °C CT (a); big CGS and 45 °C CT (b); small CGS and 36 °C CT (c); small CGS and 45 °C CT (d). Fat appears red and protein appears green. The scale are 250 μm in length. The white outline indicates a mini curd particle completely surrounded by curd junctions.



Online Resource 4: Confocal laser scanning microscopy image of rennet-induced gel obtained using a 63x objective lens. Fat appears red and protein appears green in this image. The scale bar is 50 μm in length. AFG = aggregates of fat globule, CFG = coalesced fat globule.



Online Resource 5: Confocal laser scanning microscopy (left) and cryo-scanning electron microscopy (right) images showing curd grain junctions in cheese samples. For CLSM image, fat appears red and protein appears green. Scale bars of both images are 50 µm in length. White arrows indicate the presence of crystalline inclusions of calcium phosphate. CJ = curd junction.



Online Resource 6: Cryo-scanning electron microscopy images showing curd grain junctions and crystalline inclusions of calcium phosphate in cheese samples. Cheesemaking treatments were coded as: big CGS and 36 °C CT (a); big CGS and 45 °C CT (b); small CGS and 36 °C CT (c); small CGS and 45 °C CT (d). Scale bars of images 1, 2 and 4 are 300 μm and of image 3 is 200 μm in length.



Minerva Access is the Institutional Repository of The University of Melbourne

Author/s:

Aldalur, A; Ong, L; Bustamante, MÁ; Gras, SL; Barron, LJR

Title:

Impact of processing conditions on microstructure, texture and chemical properties of model cheese from sheep milk

Date:

2019-07-01

Citation:

Aldalur, A., Ong, L., Bustamante, M. Á., Gras, S. L. & Barron, L. J. R. (2019). Impact of processing conditions on microstructure, texture and chemical properties of model cheese from sheep milk. *Food and Bioproducts Processing*, 116, pp.160-169.

<https://doi.org/10.1016/j.fbp.2019.05.003>.

Persistent Link:

<http://hdl.handle.net/11343/238435>

File Description:

Accepted version